

The Color Antisymmetric Ghost Propagator and One-Loop Vertex Renormalization

Sadataka FURUI

*School of Science and Engineering, Teikyo University
Utsunomiya 320-8551, Japan*

(Received September 19, 2007)

The color matrix elements of the ghost triangle diagram that appears in the triple gluon vertex and the ghost-ghost-gluon triangle diagram that appears in the ghost-gluon-ghost vertex are calculated. The ghost-ghost-gluon triangle contains a loop consisting of two color diagonal ghosts and one gluon and a loop consisting of two color antisymmetric ghosts and one gluon. Consequently, the pQCD argument in the infrared region based on the one particle irreducible diagram should be modified.

Implications for the Kugo-Ojima color confinement and the QCD running coupling are discussed.

§1. Introduction

In 1971, 't Hooft¹⁾ showed that in massless Yang-Mills field theory, non-gauge invariant regulator fields can be incorporated, provided that in the limit of high regulator mass the gauge invariance can be restored by means of a finite number of counter terms including ghost fields and longitudinally polarized gauge fields. After this work, Taylor²⁾ pointed out that if the charge carried by the ghost and the gauge field are the same, the Ward identity in QED, i.e. $Z_1/Z_2 = 1$, where Z_1 is the vertex renormalization factor and Z_2 is the matter field wave function renormalization factor, can be extended to QCD as $Z_1/Z_3 = Z_{\bar{\psi}\psi A}/Z_\psi$, where Z_3 is the gluon wave function renormalization factor, Z_ψ is the matter field wave function renormalization factor, and $Z_{\bar{\psi}\psi A}$ is the vertex renormalization factor of the matter field.

In these arguments, vertices at tree level are considered, and the ghost propagators were assumed to be color diagonal. The ghost propagator is defined as the Fourier transform (FT) of the matrix element of the inverse Faddeev-Popov operator,

$$\begin{aligned} FT[D_G^{ab}(x, y)] &= FT\langle \text{tr}(\Lambda^a \{(\mathcal{M})^{-1}\}_{xy} \Lambda^b) \rangle \\ &= \delta^{ab} D_G(q^2), \end{aligned}$$

where $\mathcal{M} = -\partial_\mu D_\mu$, and $\{ \}_{xy}$ represents the matrix value. We define the ghost dressing function $G(q^2)$ as $q^2 D_G(q^2)$. In the Dyson-Schwinger (DS) approach, $G(q^2)$ at 0 momentum behaves as $\sim (q^2)^{-\kappa}$, and that of the gluon dressing function $Z(q^2)$ behaves as $\sim (q^2)^{2\kappa}$.³⁾

In lattice simulations,^{4),5),6),7)} we calculated the overlap to obtain the color

diagonal ghost propagator,

$$D_G(q) = \frac{1}{N_c^2 - 1} \frac{1}{V} \text{tr} \left\langle \delta^{ab} (\langle \Lambda^a \cos q \cdot x | f_c^b(x) \rangle + \langle \Lambda^a \sin q \cdot x | f_s^b(x) \rangle) \right\rangle,$$

and the color antisymmetric ghost propagator

$$\phi^c(q) = \frac{1}{\mathcal{N}} \frac{1}{V} \text{tr} \left\langle f^{abc} (\langle \Lambda^a \cos q \cdot x | f_s^b(x) \rangle - \langle \Lambda^a \sin q \cdot x | f_c^b(x) \rangle) \right\rangle,$$

where $\mathcal{N} = 2$ for $SU(2)$ and 6 for $SU(3)$. Here, $f_c^b(x)$ and $f_s^b(x)$ represent the solution $f^b(x) = \mathcal{M}[U]^{-1} \rho^b(x)$, where U is the lattice link variable, with $\rho_c^b(x) = \frac{1}{\sqrt{V}} \Lambda^b \cos q \cdot x$ and $\rho_s^b(x) = \frac{1}{\sqrt{V}} \Lambda^b \sin q \cdot x$, respectively. We normalize the $SU(3)$ generator Λ^a as $\Lambda^a = \frac{\lambda}{\sqrt{2}}$, where λ is that defined by Gell-Mann. In our notation, we have $\text{tr} \Lambda^a \Lambda^b = \delta^{ab}$.

Lattice studies of the color antisymmetric ghost propagator in quenched $SU(2)$ ⁸⁾ and unquenched $SU(3)$ ^{5),6),7)} were motivated by analysis in the local composite operator (LCO) approach based on symmetry under the BRST (Becchi, Rouet, Stora and Tyutin) transformation.^{9),11)} The presence of $\langle f^{abc} \bar{c}^b c^c \rangle$ condensates was expected to manifest itself in the color anti-symmetric ghost propagator. The ghost condensates, as the on-shell BRST partner of A^2 condensates, were also discussed in Ref.¹⁰⁾ In the study of unquenched $SU(3)$,^{5),6),7)} the modulus of the color antisymmetric ghost propagator is found to be relatively large, and its infrared singularity, characterized by $\alpha'_G \sim 0.9$, is larger than that of the color diagonal ghost propagator $\alpha_G \sim 0.25$.⁵⁾ However, analysis of quenched $SU(3)$ on a 56^4 lattice⁷⁾ showed that the modulus of the color antisymmetric ghost propagator is small and its sample variation is large.

These data suggest that the ghost propagators of $SU(2)$ and $SU(3)$ are qualitatively different, although the gluon propagators of the two are similar, and that the presence of the dynamical quark affects the color antisymmetric ghost propagator.

In the momentum subtraction scheme (\widetilde{MOM} scheme), the running couplings in the Coulomb gauge and in the Landau gauge are calculated as the product of color diagonal ghost dressing function squared and the gluon propagator. The running coupling in the Landau gauge is

$$\alpha_s(q) = q^6 D_G(q)^2 D_A(q),$$

where $D_A(q)$ is the gluon propagator in 4-dimensional space, and that in the Coulomb gauge is

$$\alpha_I(\mathbf{q}) = \mathbf{q}^5 D_G(\mathbf{q})^2 D_A^{tr}(\mathbf{q}),$$

where $D_A^{tr}(\mathbf{q})$ is the 3-dimensional transverse gluon propagator.

In the Coulomb gauge, the color-Coulomb potential defines another running coupling $\alpha_{Coul}(\mathbf{q}) = \frac{11N_c - 2N_f}{12N_c} q^2 V_{Coul}(\mathbf{q})$. Because we do not fix A_0 , the variation of $\alpha_{Coul}(\mathbf{q})$ in the infrared region is large.

We observed that the running coupling in the Landau gauge, $\alpha_s(q^2)$, has a peak around 2.3, near $q = 0.4$ GeV, but it is strongly suppressed below 0.4 GeV, whereas that in the Coulomb gauge $\alpha_I(\mathbf{q})$ exhibits freezing to a constant around 3.¹²⁾ This qualitative difference is believed to be due to the difference between the ghost propagators: That in the Coulomb gauge is 3 dimensional and instantaneous, while that in the Landau gauge is 4 dimensional and propagating in the 4th direction.

In usual perturbative QCD (pQCD), a ghost is assumed to be color diagonal, which is valid at high energy. In a study of the Gribov horizon, Zwanziger introduced a real Bose (ghost) field $\phi_\mu^{ab}(x)$ and the additional action^{13),14)}

$$\begin{aligned} S &= S_{cl} + \gamma S_1 + S_2 \\ S_{cl} &= \frac{1}{4} \sum_{\mu,\nu,a} \int d^4x (F_{\mu\nu}^a(x))^2 \\ S_1 &= -(2C)^{-1} \int \int d^4x d^4y \text{tr} A_\mu(x) \mathcal{M}[A]^{-1} A_\nu(y) \\ S_2 &= \int d^4x \left(\frac{1}{2} \phi_\mu^{ab} \mathcal{M}^{bd}[A] \phi_\mu^{ad} + i\gamma^{1/2} C^{-1/2} f^{abd} \phi_\mu^{ad} A_\mu^b \right), \end{aligned} \quad (1.1)$$

in order to restrict the gauge configuration in the fundamental modular region. Here, C is the value of the $SU(3)$ Casimir operator of the fundamental representation.

In the Gribov-Zwanziger Lagrangian, the equation of motion for ϕ_μ^{ad} becomes¹⁵⁾

$$(D_\mu \phi_\nu)^{ab} = \partial_\mu \phi_\nu^{ab} f^{acd} A_\mu^c \phi_\nu^{db}, \quad (1.2)$$

and its solution is

$$\phi_\mu^{ab} = -\frac{\gamma^2}{\sqrt{2}} f^{abc} \mathcal{M}[A]^{-1} A_\mu^c. \quad (1.3)$$

When A_μ^c is replaced by $q_\mu c^c$, where c^c is the ghost field and f^{deh} is multiplied, we obtain

$$f^{deh} \phi_\mu^{ab} = -\frac{\gamma^2}{\sqrt{2}} (\delta^{ae} \delta^{bh} - \delta^{be} \delta^{ah}) \mathcal{M}[A]^{-1} q_\mu c^c. \quad (1.4)$$

The color antisymmetric ghost, $\phi^c(q)$, multiplied by the momentum q_μ and f^{deh} is similar to Zwanziger's ghost, ϕ_μ^{ab} . In an analytical one-loop calculation, based on the Gribov-Zwanziger Lagrangian, including two additional ghost field denoted by $\{\phi_\mu^{ab}, \bar{\phi}_\mu^{ab}\}$ and $\{\omega_\mu^{ab}, \bar{\omega}_\mu^{ab}\}$, infrared freezing of the running coupling $\alpha_s(q)$ was demonstrated.¹⁵⁾ Although Zwanziger's ghost, ϕ_μ^{ab} , was introduced in order to restrict the gauge configuration into the fundamental modular region, its relation to the A^2 condensates is discussed in Ref.¹⁶⁾ Although the color antisymmetric ghost multiplied by the momentum q_μ and f^{deh} and Zwanziger's ghost are different, we expect similar corrections to the infrared exponents of the gluon propagator and the ghost propagator through the color antisymmetric ghost propagator in the Landau gauge, when it is incorporated properly.

The organization of this paper is as follows. In § 2 we study the triple gluon vertex and the ghost-gluon-ghost vertex in one loop. In § 3, the contribution of the

ghost loop in the gluon propagator is investigated, and in § 4, the contribution of the gluon-ghost-ghost loop in the ghost propagator is studied. Discussion of the quark-gluon vertex, the Kugo-Ojima confinement parameter and QCD running coupling is given in §§ 5 and 6. A conclusion and discussion on the outlook are given in § 7.

§2. The triple gluon vertex and the ghost-gluon-ghost vertex

In this section we study the contribution of the color antisymmetric ghost propagator in the triple gluon vertex and the ghost-gluon-ghost vertex.

The triple gluon vertex defined in Fig. 1 in the pQCD is given by the tree-level diagram (Fig. 2), ghost loop diagram (Fig. 3) and the gluon loop diagram (Fig. 4)

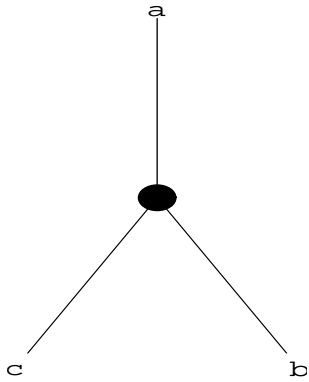


Fig. 1. The triple gluon vertex.

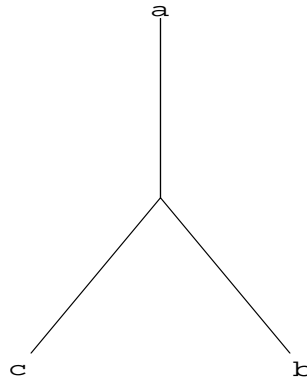


Fig. 2. The bare triple gluon vertex.

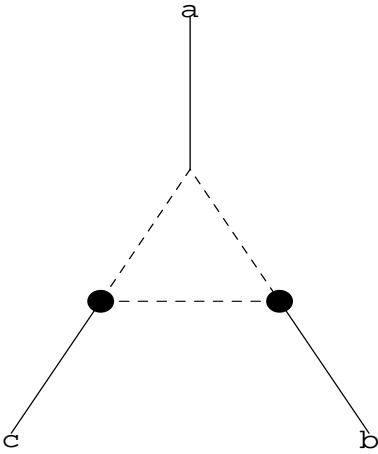


Fig. 3. The dressed triple gluon vertex. The dashed line represents a ghost and the thin line a gluon.

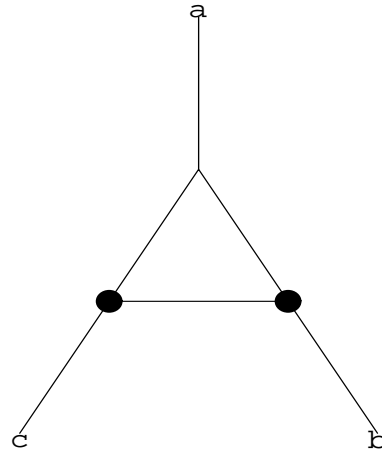


Fig. 4. The triple gluon vertex. The thin lines represent gluons.

The color indices of the ghost loop in the triple gluon vertex are assigned as in Fig. 5. We express the ghost propagator, which is assigned as d , as a combination

of the color diagonal and color antisymmetric pieces:

$$\delta^{a''c''} D_G(k) + 2f^{a''c''d} \phi_d(k). \quad (2.1)$$

The same combination is assumed for the ghost assigned as h . The color factor

$$f^{a''a'a} f^{b''b'b} f^{c''c'c} \quad (2.2)$$

is multiplied at the three edges of the triangle.

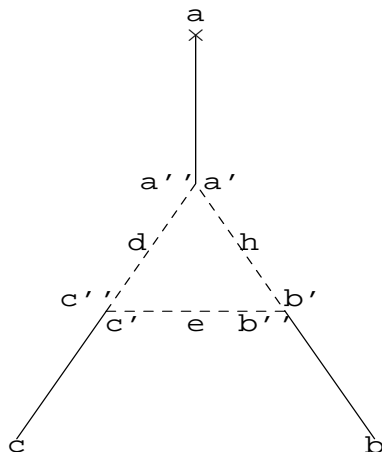


Fig. 5. The triple gluon vertex. The dashed line represents a ghost and the thin line is a gluon.

The ghost-gluon-ghost vertex is expressed as in Fig. 6 and its tree-level diagram is given in Fig. 7. At the one-loop level, the ghost-ghost-gluon loop shown in Fig. 8 contributes. The assignment of the color indices is shown in Fig. 9.

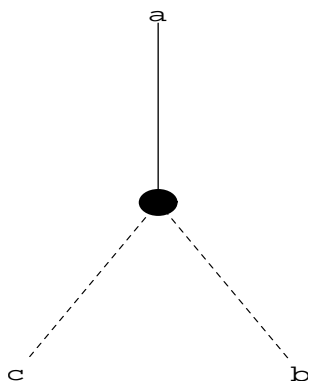


Fig. 6. The gluon-ghost-ghost vertex. The dashed line represents a ghost and the thin line a gluon.

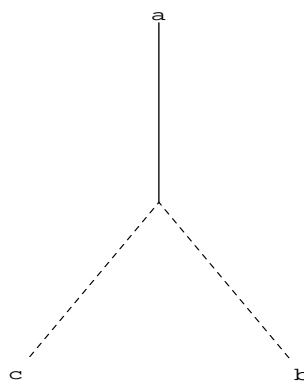


Fig. 7. The gluon-ghost-ghost vertex. The dashed line represents a ghost and the thin line a gluon.

In the calculation of the color matrix element of the one loop vertex diagram in Figs. 5 and 9, we fix a, b, c and carry out a summation over the color indices $a', a'', b', b'', c', c'', d, e, h$. The matrix elements of the quark gluon vertices are proportional to f^{abc} , which are given by

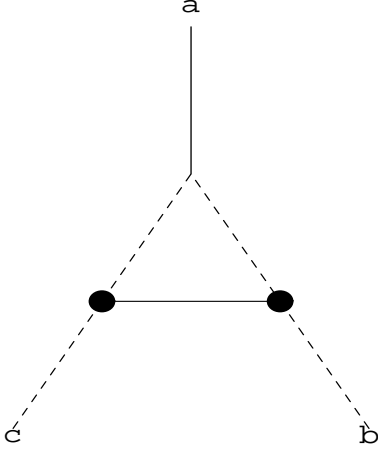


Fig. 8. The gluon-ghost-ghost vertex. The dashed line represents a ghost and the thin line a gluon.

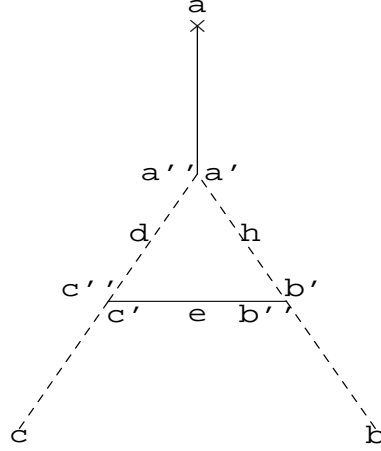


Fig. 9. The gluon-ghost-ghost vertex. The dashed line represents a ghost and the thin line a gluon.

- $f^{123} = 1$,
- $f^{147} = f^{246} = f^{345} = f^{516} = f^{257} = f^{637} = \frac{1}{2}$,
- $f^{458} = f^{678} = \frac{\sqrt{3}}{2}$.

Using the definitions $D_{c'b'} \equiv D_e$, $D_{a'b'} \equiv D_h$ and $D_{a'c'} \equiv D_d$, we obtain in the case of $SU(2)$ the coefficients given in Table I. In this table, abc and deh are the $SU(2)$ color indices, $D_h D_d D_e$ represents all color diagonal $D_h \phi_d \phi_e$, and $D_e \phi_h \phi_d$ represent one propagator assigned as D_h or D_e are color diagonal but the rest are color antisymmetric.

When deh are not elements of the Cartan subalgebra, there appear terms proportional to $\phi\phi\phi$, but the coefficient is purely imaginary, and both plus sign terms and minus sign terms appear, and they cancel.

abc	deh	$D_h D_d D_e$	$D_h \phi_d \phi_e$	$D_d \phi_e \phi_h$	$D_e \phi_h \phi_d$
123	333	-1	-4	0	0

Table I. The $SU(2)$ color matrix elements of the ghost triangle diagram.

In the case of $SU(3)$, we obtain the coefficients which are to multiply f^{abc} , as in Table II. The gluon that has the color index in the Cartan subalgebra couples with a pair of color antisymmetric ghost propagators and the contribution has the same sign as the contribution of the gluon that couples with a pair of color diagonal ghost propagators.

The qualitative difference between the color matrix elements of $SU(2)$ and $SU(3)$ comes from the anomaly cancelling equation of the triangle diagram

$$\text{tr}\{\{A^a, A^b\}A^c\} = 0, \quad (2.3)$$

where $\{\}$ represents the anti-commutator, is satisfied for $SU(2)$ but not for $SU(3)$.

abc	deh	$D_h D_d D_e$	$D_h \phi_d \phi_e$	$D_d \phi_e \phi_h$	$D_e \phi_h \phi_d$
123	888	-1.5	-1.5	1.5	1.5
	333	-1.5	-4.5	0	0
	833	-1.5	0	-0.5	0
	383	-1.5	0	0	-0.5
	338	-1.5	-4.5	0	0
	838	-1.5	0	0	1.5
	883	-1.5	-1.5	0	0
	388	-1.5	0	1.5	0
147	888	-1.5	0	0	1.5
	333	-1.5	-1	1	-0.5
	338	-1.5	-1	0	$-\sqrt{3}/2$
	383	-1.5	$-\sqrt{3}$	$-\sqrt{3}$	-0.5
	833	-1.5	0	1	$\sqrt{3}/2$
	883	-1.5	0	$-\sqrt{3}$	$\sqrt{3}/2$
	838	-1.5	0	0	1.5
	388	-1.5	$-\sqrt{3}$	0	$\sqrt{3}/2$
458	888	-1.5	4.5	0	0
	333	-1.5	-1.5	1	1
	338	-1.5	-1.5	0	0
	383	-1.5	$-\sqrt{3}/2$	$-\sqrt{3}$	1
	833	-1.5	$-\sqrt{3}/2$	1	$-\sqrt{3}$
	388	-1.5	$-\sqrt{3}/2$	0	0
	883	-1.5	-4.5	$-\sqrt{3}$	$-\sqrt{3}$
	838	-1.5	$-\sqrt{3}/2$	0	0
453	888	-1.5	-1.5	0	0
	333	-1.5	-4.5	1	1
	833	-1.5	$\frac{3\sqrt{3}}{2}$	1	$\sqrt{3}$
	383	-1.5	$-\frac{3\sqrt{3}}{2}$	$\sqrt{3}$	1
	338	-1.5	-4.5	$-2\sqrt{3}$	$-2\sqrt{3}$
	838	-1.5	$\frac{3\sqrt{3}}{2}$	$-2\sqrt{3}$	0
	883	-1.5	-1.5	$\sqrt{3}$	$\sqrt{3}$
	388	-1.5	0	$-\frac{3\sqrt{3}}{2}$	$-2\sqrt{3}$
678	888	-1.5	-4.5	0	0
	333	-1.5	-1.5	1	1
	338	-1.5	-1.5	0	0
	383	-1.5	$\sqrt{3}/2$	$\sqrt{3}$	1
	833	-1.5	$\sqrt{3}/2$	1	$\sqrt{3}$
	388	-1.5	$\sqrt{3}/2$	0	0
	883	-1.5	-4.5	$\sqrt{3}$	$\sqrt{3}$
	838	-1.5	$\sqrt{3}/2$	0	0

Table II. The $SU(3)$ color matrix elements of the ghost triangle.

The coefficients of the $D\phi\phi$ terms of f^{458} and f^{678} differ only in their signs. When the color indices are $deh = 333$ and $abc = 123$, the same structure as in the $SU(2)$ appears. But in the case of $deh = 888$ and $abc = 147$ since f^{458} and f^{678} are the only coefficient that do not vanish when coupled to the color source 8, the color antisymmetric pair of d and e appear in the link.

In the case of the unquenched $SU(3)$ configuration with the Kogut-Susskind

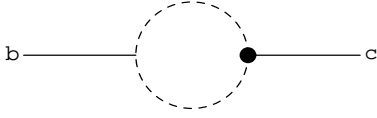


Fig. 10. The gluon propagator dressed by the ghost propagator.

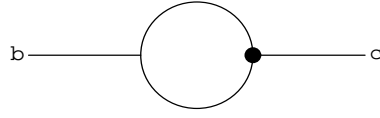


Fig. 11. The gluon propagator dressed by gluon propagator.

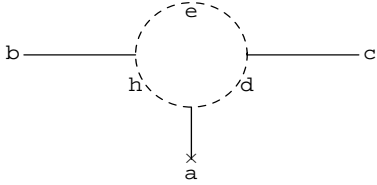


Fig. 12. The ghost loop contribution in the gluon propagator. The dashed line represents a ghost. The \times indicates the dressing of a gluon whose color index is a .

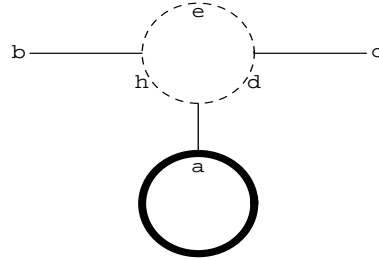


Fig. 13. The ghost loop contribution in the gluon propagator. The dashed line represents a ghost and the thick line is a quark.

fermion MILC $_f$, the ratio of the dressing function $q^2\phi(q)/G(q)$ for $q \sim 0.18$ GeV is about 0.2 and for $q \sim 0.4$ GeV is 0.08,^(6),7) while in the case of quenched $SU(2)$, the ratio for $q \sim 0.25$ GeV is about 0.1^(8),17) and for $q \sim 0.4$ GeV is 0.05 – 0.06.^(5),8),17)

§3. The ghost loop in the gluon propagator

At one-loop order, the vacuum polarization tensor that contributes to the gluon self-energy consists of a) a quark loop, b) a ghost loop (Fig. 10), c) a gluon tadpole and d) a gluon loop (Fig. 11). In b) there is a ghost-gluon-ghost vertex, and in d) there is a triple gluon vertex at two-loop order, in which the color antisymmetric ghost could contribute. In this section, we study the effect of the ghost loop on the gluon propagator.

The product of the color antisymmetric ghost propagator contributes to the ghost-loop diagram as shown in Fig. 12. There the cross indicates a coupling to the quark loop, as shown in Fig. 13, or to gluon loops. The quark loop or the gluon loop can couple to other gluons, and among the ghost propagator specified by d, e and h , one is color diagonal and the other two are color antisymmetric. The color matrix elements we calculated in the triple gluon vertex imply that if the ghost propagator that does not couple with the gluon of color index a is color diagonal and the rest are color antisymmetric, the color index a should belong to the Cartan subalgebra, in order that the matrix element becomes real.

But because other gluons can couple to the quark loop, the color index a is not necessarily in the Cartan subalgebra. The propagator is proportional to f^{abc} , and since the signs of the color matrix element given in Table II are random, its contribution is expected to be small, and thus the color mixing of gluons should be small. Lattice simulations also indicate that the gluon propagator is diagonal in the

color.

§4. The ghost-ghost-gluon loop in the ghost propagator

At one-loop order, the ghost self-energy is given by the gluon-ghost loop shown in Fig. 14.

At two-loop order, the ghost-ghost-gluon loop contributes in such a manner that a pair of color antisymmetric ghost propagator and the gluon propagator are incorporated. We consider the production of the color antisymmetric ghost pair from a gluon of color index a . The propagator shown in Fig. 15 is proportional to f^{abc} , and its trace vanishes. However, the product of these propagators shown in Fig. 16 does not vanish, and they contribute to the dressing of the external ghosts of the ghost-gluon-ghost vertex.



Fig. 14. The ghost propagator.

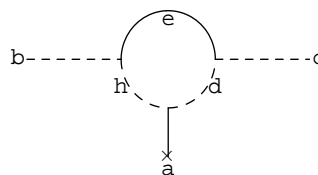


Fig. 15. The dressing of the ghost propagator by the gluon. The dashed line is a ghost the thin line is a gluon. The \times indicates dressing of a gluon in Cartan subalgebra.

When the gluon with color index a can be treated as a background field that couples to a quark loop, as shown in Fig. 17 the color antisymmetric ghost propagator contributes. In contrast to the gluon propagator, the color mixing of the ghost is not ruled out from the lattice simulations.

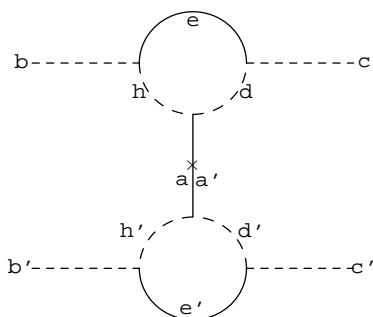


Fig. 16. The two-ghost propagator. The \times indicates a gluon of color indices $a = a'$ in the Cartan subalgebra.

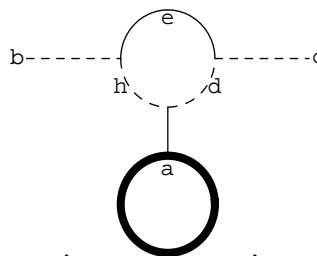


Fig. 17. The dressing of the ghost propagator by the gluon. The dashed line represents a ghost the thin line a gluon, and the thick line a quark.

The dressing of the ghost propagator by the gluon is depicted in Fig. 14. The integral is given by

$$d(b, c) = \int \frac{d^4 q}{(2\pi)^4} \delta^{bc} \left(\frac{\delta_{\mu\nu} q_\mu q_\nu}{(p-q)^2 q^{2(1+\kappa)}} - \frac{q_\mu q_\nu (p-q)_\mu (p-q)_\nu}{(p-q)^4 q^{2(1+\kappa)}} \right) Z_3((p-q)^2). \quad (4.1)$$

When $Z_3((p-q)^2)$ is taken as a constant, the formulae in Ref.²²⁾ give

$$d(b, c) \propto K_2(1+\kappa, 1, p)p^2 - (K_2(1+\kappa, 2, p)p^4 - 2L_2(1+\kappa, 2, p)p^4 + M_3(1+\kappa, 2, p)p^4), \quad (4.2)$$

where

$$\begin{aligned} \int d^4 q \frac{q_\mu q_\nu}{q^{2a} (P-q)^{2b}} &= K_1(a, b, p) p_\mu p_\nu + K_2(a, b, p) p^2 \delta_{\mu\nu}, \\ \int d^4 q \frac{q_\mu q_\nu q_\rho}{q^{2a} (p-q)^{2b}} &= L_1(a, b, p) p_\mu p_\nu p_\rho + L_2(a, b, p) p^2 (p_\mu \delta_{\nu\rho} + p_\nu \delta_{\rho\mu} + p_\rho \delta_{\mu\nu}), \\ \int d^4 q \frac{q_\mu q_\nu q_\rho q_\sigma}{q^{2a} (p-q)^{2b}} &= M_1(a, b, p) p_\mu p_\nu p_\rho p_\sigma \\ &+ M_2(a, b, p) p^2 (\delta_{\mu\nu} p_\rho p_\sigma + \delta_{\mu\rho} p_\nu p_\sigma + \delta_{\mu\sigma} p_\rho p_\mu + \delta_{\nu\rho} p_\mu p_\sigma + \delta_{\nu\sigma} p_\rho p_\mu + \delta_{\rho\sigma} p_\mu p_\nu) \\ &+ M_3(a, b, p) p^4 (\delta_{\mu\nu} \delta_{\rho\sigma} + \delta_{\mu\rho} \delta_{\nu\sigma} + \delta_{\mu\sigma} \delta_{\rho\nu}). \end{aligned} \quad (4.3)$$

According to the ansatz of the DS equation, the exponent of the ghost dressing function is given by $\kappa \sim \alpha_G$ and it is related to the exponent of the gluon dressing function α_D as $-2\kappa \sim \alpha_D$.⁴⁾ When $\kappa = 0.5$, corresponding to an infrared finite gluon propagator, the integral becomes

$$\delta^{bc} d(b, c) = -\frac{6.26379}{(p^2)^{0.5}} - \left(\frac{6.57974}{(p^2)^{0.5}} - 2 \frac{3.94784 p^2}{(p^2)^{0.5}} - \frac{1.12795 p^4}{(p^2)^{0.5}} \right) \quad (4.4)$$

Analysis of the exponent of the gluon dressing function of lattices with a long time axis is given in Ref.¹⁸⁾ In reality, κ in the infrared and ultraviolet regions could be different, and the above numerical values should be regarded as simple estimations.

The loop integral of the ghost-ghost-gluon triangle is given by

$$\begin{aligned} I(p, a, b, c) &= \int \frac{d^4 q}{(2\pi)^4} \left(\delta_{\mu\nu} - \frac{(p-q)_\mu (p-q)_\nu}{(p-q)^2} \right) \frac{Z_3((p-q)^2)}{(p-q)^2} \\ &\times \left(\frac{\delta^{a''c''}}{q^{2(1+\kappa)}} + 2i f^{a''c''d} \phi_d(q) \right) (-g f^{a''aa'} q_\mu) \\ &\times \left(\frac{\delta^{b'a'}}{q^{2(1+\kappa)}} + 2i f^{b'a'h} \phi_h(q) \right) (-g f^{b''bb'} q_\nu) \\ &\times \sum_x (\text{loop term})(t^a)_{xx}. \end{aligned} \quad (4.5)$$

where the quark loop contribution is expressed as the loop term.

abc	dh	$D_h D_d D_{Ae}$	$D_{Ae} \phi_h \phi_d$
321	88	1.5	-1.5
	33	1.5	-4.5
	83	1.5	0
	38	1.5	0
854	88	1.5	-4.5
	33	1.5	-1.5
	83	1.5	$\sqrt{3}/2$
	38	1.5	$\sqrt{3}/2$
876	88	1.5	-4.5
	33	1.5	-1.5
	83	1.5	$-\sqrt{3}/2$
	38	1.5	$-\sqrt{3}/2$

Table III. The $SU(3)$ color matrix elements of the ghost-ghost-gluon triangle.

The color matrix elements are given in Table IV, where D_{Ae} indicates the color diagonal gluon propagator. The coherent contribution, $D_e \phi \phi$ from $dh=88$ and 33 suggests that color mixing occurs in the infrared region. The contribution of the color antisymmetric ghost propagator would be enhanced in an unquenched lattice simulation, in which case the quark loop becomes a source of the color antisymmetric pair.

The exponent of the color diagonal ghost dressing function α_G is ~ 0.25 ,^{5),4)} and that of the color antisymmetric ghost dressing function defined at $q \sim 0.4$ GeV is $\alpha'_G \sim 0.9$.⁶⁾ By using the formulae in Ref.²²⁾ and assuming $Z_3((p-q)^2)$ is constant in the relevant integration region, we obtain

$$\begin{aligned}
I(p, a, b, c) &\propto f^{abc} (c_1 K_2(2(1+\kappa), 1, p) p^2 + c_2 K_2(2(1+\kappa'), 1, p) p^2) \\
&- (c_1 (K_2(2(1+\kappa), 2, p) p^4 - 2L_2(2(1+\kappa), 2, p) p^4 + M_3(2(1+\kappa), 2, p) p^4) \\
&- (c_2 (K_2(2(1+\kappa'), 2, p) p^4 - 2L_2(2(1+\kappa'), 2, p) p^4 + M_3(2(1+\kappa'), 2, p) p^4) \quad (4.6)
\end{aligned}$$

where c_1 is the color matrix element of $D_{Ae} D_h D_d$, and c_2 is the color matrix element of $D_{Ae} \phi_h \phi_d$. Using $\kappa = 0.5$ for D_h, D_d and $\kappa' = 0.9$ for ϕ_h, ϕ_d , we obtain

$$\begin{aligned}
I(p, a, b, c) &\propto f^{abc} \left(c_1 \left(-\frac{\infty}{p^2} \right) + c_2 \left(-\frac{6.1196}{p^{2.8}} \right) \right. \\
&- \left(c_1 \left(-\frac{\infty}{p^2} - 2\frac{\pi^2}{4p^2} + \frac{\pi^2}{16p^2} \right) \right) \\
&- \left. \left(c_2 \left(-\frac{2.203}{p^{3.8}} - 2\frac{8.81215}{p^{3.8}} + \frac{2.03985}{p^{3.8}} \right) \right) \right). \quad (4.7)
\end{aligned}$$

We remark that the divergent terms cancel.

The dressed ghost propagator can be incorporated into the ghost loop in the gluon propagator, as shown in Fig. 18, and thereby modify the infrared behavior of the gluon propagator in the lattice Landau gauge.

The loop of quarks in the fundamental representation yields $\text{tr}(t^{c'} t^{c''}) = \delta^{c', c''} \frac{1}{2}$.

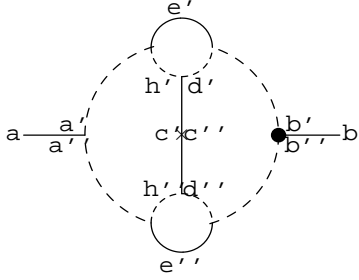


Fig. 18. The gluon propagator with a ghost loop. The dashed line represents a ghost, the thin line a gluon. The \times indicates dressing of the gluon in Cartan subalgebra.

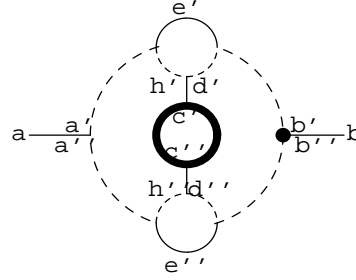


Fig. 19. The gluon propagator with a ghost loop and quark loop contributions. The dashed line represents a ghost, the thin line a gluon, and the thick line a quark.

c—ab	11	22	33	44	55	66	77	88
3	-0.25	-0.25	2.25	0.5	0.5	0.5	0.5	0.75
8	0.75	0.75	0.75	0	0	0	0	2.25

Table IV. Color matrix elements of the gluon propagator.

The sum of the color indices becomes

$$2g(a, b, c', c'') = \sum_{a', a'', b', b''} \delta^{c', c''} f^{aa'a''} f^{bb'b''} f^{c'a'b'} f^{c''a''b''}. \quad (4.8)$$

This gives $4.5\delta^{ab}$. The $D_{Ae}\phi_h\phi_d$ loop contribution, denoted by c_2 , exists only when $c', c'' = 3, 8$. There is no restriction to the $D_{Ae}D_hD_d$ loop contribution denoted by c_1 , but the infrared singularity of the c_2 term is stronger than that of the c_1 term.

§5. The quark-gluon vertex

The quark-gluon vertex is calculated from the longitudinal photon quark coupling

$$q_\mu \Gamma_\mu(p, q) = G(q^2)[(1 - H(q, p + q))S^{-1}(p) - S^{-1}(1 - H(q, p + q))], \quad (5.1)$$

where $G(q^2)$ is the ghost dressing function and $H(q, p + q)$ is the ghost-quark scattering kernel. In the continuum theory, the ghost-quark scattering kernel in the quark-gluon vertex is studied in Ref.¹⁹⁾ Its role in the DS approach is examined in Ref.²⁰⁾ and it is studied by lattice simulation in Ref.²¹⁾

In the quark-gluon vertex, a ghost-triangle couples with an external gluon, and two internal gluons couple to the quark, as shown in Fig.20.

The color of the external gluon is specified by a , and the two internal gluons are specified by b and c . When the ghost-quark scattering kernel is approximated by a dressed gluon exchange, the amplitude of the quark-gluon vertex becomes

$$M(p, s, a, x, y) = \int \frac{d^4k}{(2\pi)^4} \int \frac{d^4q}{(2\pi)^4}$$

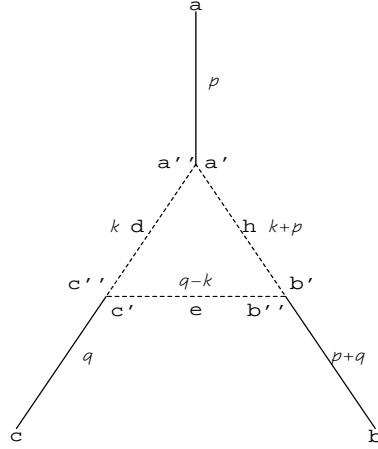


Fig. 20. The ghost triangle. The color indices of the external gluons and internal ghosts and the momentum assignments.

$$\begin{aligned}
 & \times \left(\frac{\delta^{a''c''}}{k^{2(1+\kappa)}} + 2if^{a''c''d}\phi_d(k) \right) (-gf^{a''a'd}k) \\
 & \times \left(\frac{\delta^{c'b''}}{(q-k)^{2(1+\kappa)}} + 2if^{c'b''e}\phi_e(q-k) \right) (-gf^{c''cc'}(q-k)) \\
 & \times \left(\frac{\delta^{b'a'}}{(k+p)^{2(1+\kappa)}} + 2if^{b'a'h}\phi_h(k+p) \right) (-gf^{b''bb'}(k+p)) \\
 & \times (igt^c)_{xz}(igt^b)_{zy}Z_2((s-q)^2) \frac{-i(\not{s}-\not{q})+M}{(s-q)^2+M^2} \\
 & \times (\delta_{\mu\nu} - \frac{q_\mu q_\nu}{q^2}) \frac{Z_3(q^2)}{q^2} \\
 & \times (\delta_{\eta\delta} - \frac{(q+p)_\eta(q+p)_\delta}{(q+p)^2}) \frac{Z_3((q+p)^2)}{(q+p)^2}. \tag{5.2}
 \end{aligned}$$

It is important to note that the color antisymmetric ghost does not appear as an external line, but, rather, it appears in the vertex as an internal line. The gluon dressing indicated by the cross can be contracted as $\delta^{c'c''}$ and becomes a propagator in the Cartan subalgebra. This could effectively introduce the ghost condensates effect, i.e. a choice of a specific color direction.

§6. Effects on the Kugo-Ojima color confinement parameter and the running coupling

Kugo and Ojima²³⁾ constructed a two-point function $u^{ab}(q)$ from the Lagrangian in the Landau gauge that satisfies BRST symmetry. They claimed that if its value at momentum zero is -1 , it is evidence of color confinement:

$$\begin{aligned}
(\delta_{\mu\nu} - \frac{q_\mu q_\nu}{q^2})u^{ab}(q^2) &= \frac{1}{V} \sum_{x,y} e^{-ip(x-y)} \langle \text{tr} \left(\Lambda^{a\dagger} D_\mu \mathcal{M}^{-1} [A_\nu, A^b] \right)_{xy} \rangle, \\
u^{ab}(0) &= -\delta^{ab} c.
\end{aligned} \tag{6.1}$$

In this argument and in the proof of the Slavnov-Taylor identity regarding the ratio of the vertex renormalization factor and the wave function renormalization factor,²⁴⁾

$$\frac{Z_1}{Z_3} = \frac{\tilde{Z}_1}{\tilde{Z}_3} = \frac{Z_{\bar{\psi}\psi A}}{Z_\psi},$$

the ghost propagator is assumed to be color diagonal.

The replacement

$$\langle c^a(x) \bar{c}^b(y) \rangle = D_G(x-y) \delta^{ab} + f^{abc} \phi^c(x-y) \tag{6.2}$$

does not affect the argument of the tree level, since the expectation value of $\phi(x-y)$ is 0. However, when there is a ghost color mixing of the type depicted in Fig. 15, we have

$$\langle c(A_\nu \times \bar{c}) \rangle_{1PI} \neq iq_\rho \langle (A_\rho \times c)(A_\nu \times \bar{c}) \rangle_{1PI}. \tag{6.3}$$

Thus, when we define

$$\begin{aligned}
\langle c\bar{c} \rangle &\equiv -\frac{1}{q^2 G(q^2)}, \\
\langle (A_\mu \times c)\bar{c} \rangle_{1PI} &\equiv -iq_\mu F(q^2)
\end{aligned}$$

and

$$\langle D_\mu c\bar{c} \rangle = \langle \partial_\mu c\bar{c} \rangle + \langle (A_\mu \times c)\bar{c} \rangle \equiv iq_\mu (1 + F(q^2)) \frac{1}{q^2 G(q^2)}, \tag{6.4}$$

we obtain

$$\begin{aligned}
\langle D_\mu c(A_\mu \times \bar{c}) \rangle &= \langle \partial_\mu c\bar{c} \rangle \langle c(A_\mu \times \bar{c}) \rangle_{1PI} + \langle (A_\mu \times c)(A_\nu \times \bar{c}) \rangle_{1PI} \\
&\neq (\delta_{\rho\mu} - \frac{q_\mu q_\rho}{q^2}) \langle c(A_\mu \times \bar{c}) \rangle_{1PI}.
\end{aligned} \tag{6.5}$$

In other words, although the lattice simulation confirms $G(0) = 0$,⁴⁾ there should be a contribution of the ghost propagator of the type appearing in Fig. 15 between c and \bar{c} that is not proportional to δ^{ab} , and $1 + u(0) = 1 + F(0)$ in eq.(6.4) is not necessarily equal to $G(0) = 0$.

In the S -matrix theory, the ghost intermediate state cancels the intermediate states with a non-physically polarized gluon. The longitudinal gluon with polarization vector $-ip_\mu$ couples with a set of diagrams of a given order in g and a given number of transverse gluons on mass shell, which are expressed as circles in the t' Hooft definition, and it was shown that all the contributions cancel, yielding 0, when the ghosts are color diagonal.

Our analysis suggests that if the longitudinal gluon forms a pair of color anti-symmetric ghosts and the loop intersects with the circle, the contribution remains

since the contribution of the cutoff denoted by Λ in the t' Hooft definition cancels the color-diagonal ghost contribution. This results in an artificial suppression of the ghost propagator and the QCD running coupling.

No infrared suppression occurs in $\alpha_I(\mathbf{q})$, since the longitudinal gluon polarized in the 4th direction does not contribute to the three-dimensional calculation.

The color indices of the color antisymmetric ghost pair could be ordered if there is a long-range background gluon field that couples to the pair. In this case, Eq.(6.5) would be satisfied and the Kugo-Ojima parameter c would become close to 1.

There is no direct proof that the quark loop introduces ordering, but the difference between the Binder cumulants of the color antisymmetric ghost propagator of the quenched simulation and the unquenched simulations^{5),6),7)} strongly suggests this effect. The temperature dependence of the parameter c ⁷⁾ could also be explained by this mechanism.

§7. Discussion and outlook

We investigated whether the deviation of the Kugo-Ojima parameter c from 1 and the infrared suppression of the effective coupling $\alpha_s(q)$ in the Landau gauge could be due to the color antisymmetric ghost propagator.

In the case of the Coulomb gauge, the ghost dressing function is three dimensional, no dissipation of the flow occurs and the running coupling freezes.

The lattice Landau gauge results show some discrepancies from the results of the DS equation with regard to the infrared exponents of the ghost propagator and the gluon propagator. We investigated the possibility that this discrepancy comes from the color-mixing of the ghost propagator induced by the ghost-gluon-ghost triangle diagram. A study employing the DSE is left as a future project.

The color antisymmetric ghost pair couples to a gluon whose color is in the Cartan subalgebra. The lattice data suggest that the gluon in the Cartan subalgebra couples with a dynamical quark loop, and this introduces a difference between the color antisymmetric ghost propagator of the quenched configurations and that of the unquenched configurations.

We also studied the contribution of ghost triangle diagram in the quark-gluon vertex. For the estimation of the latter effect, it is necessary to perform a two-loop calculation, and this is left to a future.

Acknowledgements

The main part of this work was done at the Department of Theoretical Physics of University of Graz in August 2007. The author thanks Kai Schwenzer and Reinhard Alkofer for helpful and enlightening discussions in Graz and Hideo Nakajima for the collaboration in the lattice simulation cited in this paper. Thanks are also due to the Austrian Academic Exchange Service for their support during the author's stay in Graz and the Japan Society for the Promotion of Science (JSPS) for support through the Scientist Exchange Program that enabled the collaboration.

References

- 1) G. 't Hooft, Nucl. Phys. **B33**(1971), 173.
- 2) J.C. Taylor, Nucl. Phys. **B33** (1971), 436.
- 3) R. Alkofer and L. von Smekal, Phys. Rep. **353**(2001),281; hep-ph/0007355.
- 4) S. Furui and H. Nakajima, Phys. Rev. **D69**(2004),074505.
- 5) S. Furui and H. Nakajima, Phys. Rev. **D73**(2006), 094506; hep-lat/0612009.
- 6) S. Furui and H. Nakajima, Br. J. Phys.**37** (2007),186.; hep-lat/0609024.
- 7) S. Furui and H. Nakajima, Phys. Rev. **D76**(2007),054509; hep-lat/0612009.
- 8) A. Cucchieri, T. Mendes and A. Mihara, Phys. Rev. **D72** (2005),094505; hep-lat/0408034.
- 9) D. Dudal et al., J. High Energy Phys. **0306**(2003), 003.
- 10) K. I. Kondo, Phys. Lett. **B514**(2001),335; hep-th/0105299.
- 11) V. E. R. Lemes, M. S. Sarandy and S. P. Sorella, Ann. of Phys. **308** (2003),1; hep-th/0210077
- 12) S. Furui and H. Nakajima, PoS (Lattice2007)(2007),301; arXiv:0708.1421
- 13) D. Zwanziger, Nucl. Phys. **B323**(1989),513.
- 14) D. Zwanziger, Nucl. Phys. **B412**(1994),657.
- 15) J. A. Gracey, J. High Energy Phys. **05**(2006), 052; hep-ph/0605077.
- 16) D. Dudal, R.F. Sobreiro, S.P. Sorella and H. Verschelde, Phys. Rev. **D72**(2005),014016 ;hep-th/0502183.
- 17) J. C. R. Bloch, A. Cucchieri, K. Langfeld and T. Mendes, Nucl. Phys. B(Proc. Supp.)**119**(2003),736; hep-lat/0209040.
- 18) O. Oliveira and P. Silva, Br. J. Phys.**37**(2007),201.
- 19) H. Pagels, Phys. Rev. **D15**(1977), 2991.
- 20) C.S. Fischer and R. Alkofer, Phys. Rev. **D67**,094020 (2003).
- 21) J. Skullerud and A. Kizilersü, J. High Energy Phys. **09**(2002), 013; hep-ph/0205318.
- 22) A. Alkofer, C. S. Fischer, H. Reinhardt and L. von Smekal, Phys. Rev. **D68**(2003),045003; hep-th/0304134.
- 23) T. Kugo and I. Ojima, Prog. Theor. Phys. Suppl. No. 66(1979), 1.
- 24) T. Kugo, hep-th/9511033.